JOURNAL OF PROPULSION AND POWER
Vol. 25, No. 3, May–June 2009

Adaptive Instability Suppression Controls Method for Aircraft Gas Turbine Engine Combustors

George Kopasakis,* John C. DeLaat,† and Clarence T. Chang‡
NASA John H. Glenn Research Center at Lewis Field, Cleveland, Ohio 44135

DOI: 10.2514/1.36777

An adaptive controls method for instability suppression in gas-turbine engine combustors has been developed and successfully tested with a realistic aircraft engine combustor rig. This testing was part of a program that demonstrated, for the first time, successful active combustor instability control in an aircraft gas-turbine enginelike environment. The controls method is called adaptive sliding phasor averaged control. Testing of the control method has been conducted in an experimental rig with different configurations designed to simulate combustors with instabilities of about 530 and 315 Hz. Results demonstrate the effectiveness of this method in suppressing combustor instabilities. In addition, a dramatic improvement in suppression of the instability was achieved by focusing control on the second harmonic of the instability. This is believed to be due to coupling in the form of energy exchange between different frequency modes in the combustor. These results may have implications for future research in combustor instability control.

I. Introduction

COMBUSTOR instability can limit the operating range of aeropropulsion engines. These instabilities are typically the result of the coupling of the fluctuating heat release [1] with the lightly damped acoustics of the combustion chamber. The exact mechanisms involved in this coupling are not well understood and different hypotheses exist as to its precise nature [2]. Furthermore, avoiding these combustion-driven pressure oscillations becomes even more important as modern engines are pushed to operate ever closer to the stability limit. For example, although lean combustion is shown to be advantageous for reducing emissions of nitrogen oxides (NO_x), lean-burning low-emissions combustors also have an increased susceptibility to instabilities. Designing engines to operate at stable conditions is always good practice, but this is often not enough to deal with exceptions such as abnormal conditions and transients. Active combustion control is a promising technique to deal with these exceptions.

Combustor instability suppression presents a challenging problem for controls design due primarily to the large dead time phase delay (of many hundreds of degrees or more) and noise in the combustion process. Besides large phase delay and noise, there are other characteristics of combustor instabilities, such as amplitude modulations and net random phase walks, which could play an important role in the control design [2,3].

A number of research efforts have attempted suppression of the thermoacoustic instability through active control [4]. The goal of these active control efforts was to reduce the energy concentrated at the instability frequency and to reduce the overall amplitude of the combustor pressure oscillations. Some active control concepts involved speaker actuation [5–11] and others involved fuel modulation [12–16]. Fuel modulation is more applicable to aircraft gas-turbine engines. Several techniques have shown some success in suppressing the frequency spectra of low-frequency instabilities, with less success in suppressing the time domain pressure fluctuations. Much of the research in the area of gas-turbine engines active combustor instability control has made use of low-pressure, gaseous fueled combustors. One exception is the work by Barooah et al. [17] that attempted to reduce pressure oscillations with the low-frequency configuration of the same liquid-fueled combustor rig described later in this paper. Even though the technique applied had some success in reducing the instability amplitude at the instability frequency, the instability energy was transferred to the frequency side lobes ("peak splitting"), and the overall amplitude of the combustor pressure oscillations was minimally reduced.

The adaptive sliding phasor averaged control (ASPAC) methodology described in this paper has successfully demonstrated instability suppression for multiple combustor rig configurations. The ASPAC method was first applied to control a high-frequency rig configuration (HFRC). These early results, presented in [18], demonstrated the effectiveness of the methodology in reducing the combustor pressure oscillations at the instability frequency. This testing, which included concurrent testing of an alternate control method, represented the first known demonstration of actively controlled, high-frequency, thermoacoustic instabilities in a realistic aircraft gas-turbine engine combustor rig (as reported in [19] and described in [18,20,21]). Later, control was attempted on a low frequency rig configuration (LFRC) that was assembled to further test and verify the control methodology. As will be shown, the LFRC exhibited a very coherent instability compared to the HFRC. (The actual engine instability, on which the HFRC design was based, exhibited instability coherence somewhere between the LFRC and the HFRC.) The ASPAC controller was also successful in suppressing this LFRC's coherent instability. Finally, due to a previously reported coupling mechanism [18,22] involving the harmonics of the instability, control was then focused on the second harmonic of the instability. This approach produced superior results.

This paper describes the development of the ASPAC controller and the results of testing the controller with a combustor instability rig. The paper is organized as follows. A description of the combustor rig is given that includes comparisons of the instabilities of the HFRC, the LFRC, and that of a developmental aircraft gas-turbine engine. This is followed by a description of the combustor instability behavioral model and the development of the control methodology. Then, test results are presented for the HFRC and the LFRC, including harmonic control and its implications, followed by some attempts to explain the phenomena observed during testing and their possible root causes. The paper concludes with areas of future research interests.

Received 22 January 2008; revision received 11 December 2008; accepted for publication 10 January 2009.

*Senior Research Engineer, Controls and Dynamics Branch, 21000 Brookpark Road. Member AIAA.
†Senior Research Engineer, Controls and Dynamics Branch, 21000 Brookpark Road. Senior Member AIAA.
‡Senior Research Engineer, Combustion Branch, 21000 Brookpark Road.

II. Experimental Hardware Description

A. Combustor Instability Rig

To focus control development toward realistic combustion instabilities in aeronautics, a single-nozzle research combustor rig that replicates an aircraft gas-turbine engine combustor instability was designed and fabricated [23,24]. A schematic of the test rig configuration is shown in Fig. 1. The sample problem selected for this rig is an axial combustor instability that was observed during the development of a high-performance aircraft gas-turbine engine. The frequency of the observed instability in the developmental engine was about 525 Hz and the magnitude of the pressure oscillations was sufficient to cause unacceptable vibratory stresses in the turbine.

It was previously demonstrated that the combustor rig successfully replicates the axial instability observed in the engine [23]. The single-nozzle combustor rig operates at engine pressure and temperature conditions and has many of the complexities of the actual engine combustor. These include the same air-blast, two-stage fuel nozzle and swirler used in the engine, dilution/cooling, and an effusion-cooled liner. The fuel used in the combustor rig is Jet A. A venturi prediffuser and dump diffuser simulate the engine compressor exit (combustor inlet) conditions. A choked nozzle at the combustor exit simulates the engine turbine stator. The nearly choked venturi and choked exit nozzle, in addition to simulating operation inside the engine, provide acoustic isolation from the rest of the facility.

Conditions corresponding to a midpower engine condition were chosen for evaluation (combustor inlet temperature = 775°F, combustor inlet pressure = 200 psia, fuel–air ratio = 0.03). Water-cooled, nitrogen-purged dynamic pressure transducers (PCB 12x series) were used to measure the pressure oscillations inside the combustor rig. Test results (Fig. 2) established the existence of a combustor instability at about 533 Hz: approximately the same frequency as the developmental engine. The test rig apparatus, as shown in Fig. 1, is configured for the 533 Hz HFRC. The LFRC is obtained by removing the prediffuser section shown in Fig. 1 and placing it before the two quarter-wave spool sections. This has the effect of elongating the combustor by approximately 19 in. and produces an instability at about 315 Hz.

For comparison, the pressure spectrum in the actual engine and in the single-nozzle combustor rig, at comparable operating conditions for the HFRC and LFRC, is shown in Figs. 2 and 3, respectively. This comparison shows that, in terms of instability frequency and amplitude, the HFRC closely simulates the actual engine instability. In terms of instability coherence for the fundamental (i.e., instability magnitude with respect to noise), however, the engine more closely resembles the behavior of the LFRC. These two rig configurations provide essentially two control problems. The HFRC provides a high-frequency, low signal-to-noise instability problem, and the LFRC provides a lower-frequency, high-amplitude, high signal-to-noise problem.

B. Fuel Modulation Valve

For the open-loop fuel modulation testing and closed-loop instability control testing, a high-frequency fuel modulation valve was developed [21] and used. The valve is based on a magnetostrictive material actuator approximately 12 in. (30.5 cm) in length. The actuator proportionally modulated a valve opening with a linear displacement of approximately 0.010 in. (0.025 cm) from full open to full closed. The valve was typically located approximately 18 in. (45.7 cm) from the fuel injector tip. The open-loop combustor pressure response to fuel valve modulation for two different runs is shown in Fig. 4. The response was somewhat nonlinear in that larger valve commands produced a disproportionately larger response in combustor pressure. However, the response of the fuel modulation system was determined empirically to be satisfactory for open-loop testing and for closed-loop instability control. The dynamics of the aforementioned fuel modulation subsystem were not investigated further. This is, however, deemed to be an important area for future research. The fuel modulation valve also included a mean flow control component consisting of a motor and cam to maintain the mean position of the valve opening. The fuel valve control system used this mean flow control feature to keep the mean flow constant while the fuel flow was perturbed. This ensured that the results seen were due to fuel modulation and not to a change in fuel flow and/or fuel–air ratio. The correct operation of the mean flow control was verified during testing and from posttest data.

III. Combustor Instability Simulation

The overall ASPAC control design diagram is shown in Fig. 5, which includes the controller and a simulation of the combustor instability process. A reduced-order behavioral model is used to represent the combustor instability. This model consists of the flame dynamics, acoustics, and a saturation nonlinearity. With the addition of noise, this instability is self-excited, that is, it requires no input via fuel injection modulation for sustained oscillations to take place. The respective transfer functions for the flame G_F, acoustics G_A, and nonlinearity (NL) are:

$$G_F = \frac{K_F \omega_F}{s + \omega_F} \tag{1}$$

$$G_A = \frac{K_A \omega_A^2}{s^2 + 2\zeta_A \omega_A + \omega_A^2} \tag{2}$$

$$\mathrm{NL} = \tanh(p) \tag{3}$$

where p is the acoustic pressure output from the transfer function in Eq. (2). These transfer functions are similar to the ones used to simulate the combustor instability in [25].

In this simulation, the flame dynamics in Eq. (1) are represented with a first-order transfer function with $\omega_F \approx 1.1\omega_A$ and a gain $K_F = 1.2$. The acoustics transfer function dynamics in Eq. (2) correspond to an instability frequency of ~533 Hz for the HFRC or ~315 Hz for the LFRC. With $\zeta_A = 0.0707$ and $K_A = -0.25$, the coupled response between the flame and acoustics becomes oscillatory and unstable (growing with time). The purpose of the

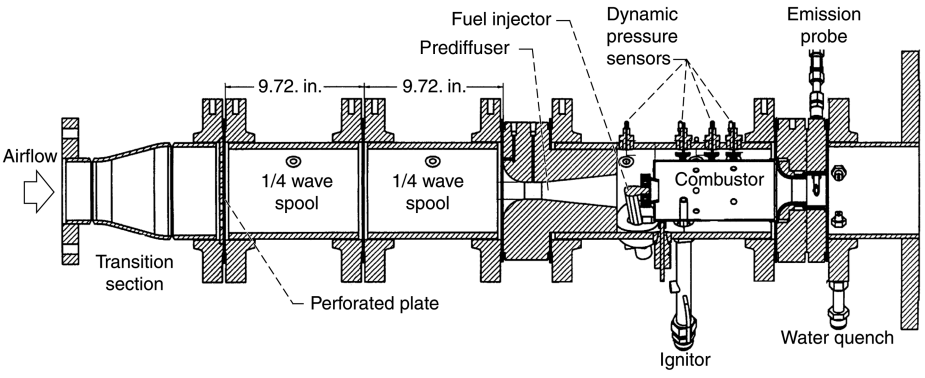

Fig. 1 Test rig configuration.

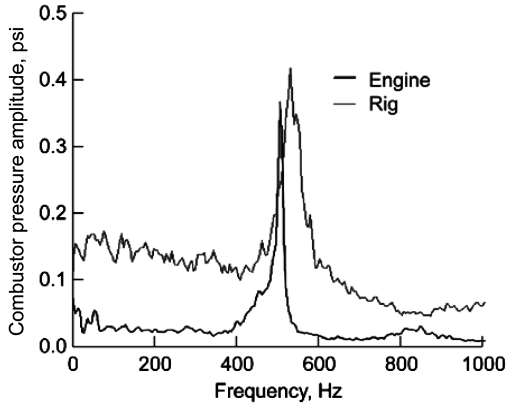

Fig. 2 Comparison of engine (midpower) and baseline combustor rig (HFRC) pressure amplitude spectra.

nonlinearity is to limit the amplitude of the instability. These choices of the transfer function parameters, with the addition of any noise magnitude other than zero, allow for self-sustained oscillations that closely approximate the combustor instability from time response measurements [2,4]. Figure 6 shows a simulation of a self-excited instability with some injected white noise added to represent the process noise in the combustor. The response is also numerically unstable in the sense that the response depends on the damping ζ_A and the sampling time T_s ($T_s = 0.0001$ s), however, the results are deterministic and repeatable.

The dynamics of the fuel valve, feed lines, injector, and heat release or flame dynamics due to the fuel modulation (G_V in Fig. 5), have been simulated with a second -order transfer function as

$$G_V = \frac{K_V \omega_V^2}{s^2 + 2\zeta_V \omega_V s + \omega_V^2} \tag{4}$$

with $K_V = 1.0$ and its natural frequency ω_V comfortably greater than ω_A so that it will not attenuate the controlled fuel modulations, with ζ_V chosen to provide a damped response.

For the filter shown in Fig. 5, two identical bandpass filters are placed in series. The purpose of these filters is 1) to pass the measured instability for control, and 2) when running the control with a simulated combustor, to simulate the large dead time phase shift found in the combustion process. Note that the feedback blocks starting from the filter to the fuel lines/combustor in Fig. 5 are all in series. Therefore, where exactly in this path the combustor delay is simulated makes no difference. This time delay phase shift amounts to approximately 760 deg for the LFRC and is significantly larger for the HFRC. The state-space model of the bandpass filter is

$$\dot{x} = Ax + Bu \qquad y = Cx \tag{5}$$

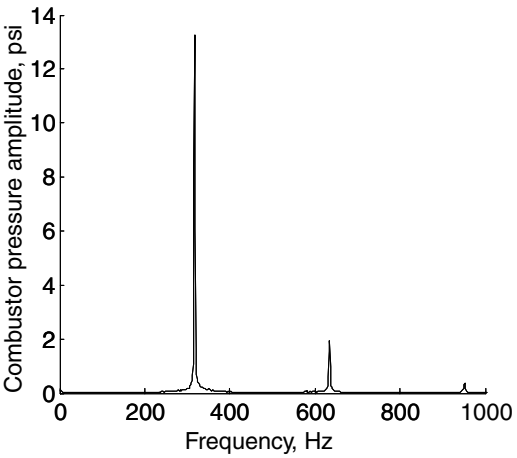

Fig. 3 Pressure amplitude spectra in extended rig configuration (LFRC).

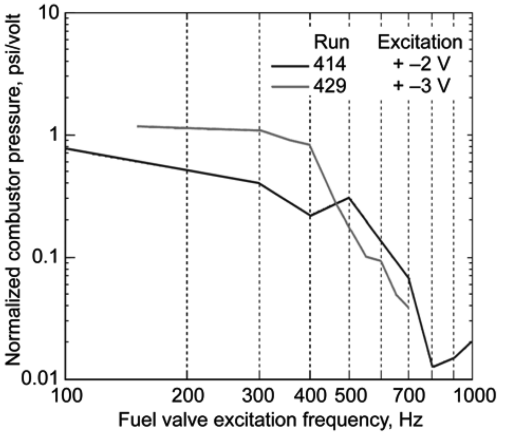

Fig. 4 Normalized combustor pressure response to perturbation of the high-frequency fuel modulation valve.

with

$$A = 1000\begin{bmatrix} -a1 & 0 & 0 & a2 & 0 & 0 \\ a1 & -a1 & -a1 & 0 & a2 & 0 \\ 0 & a1 & 0 & 0 & 0 & a2 \\ -a2 & 0 & 0 & 0 & 0 & 0 \\ 0 & -a2 & 0 & 0 & 0 & 0 \\ 0 & 0 & -a2 & 0 & 0 & 0 \end{bmatrix}$$

$$B = [\,b \quad 0 \quad 0 \quad 0 \quad 0 \quad 0\,]^T \qquad C = [\,0 \quad 0 \quad 1 \quad 0 \quad 0 \quad 0\,]$$

For this simulation, $a1_{\mathrm{HFRC}} = 0.8$, $a2_{\mathrm{HFRC}} = 3.58$, $b_{\mathrm{HFRC}} = 800$ and $a1_{\mathrm{LFRC}} = 0.4$, $a2_{\mathrm{LFRC}} = 1.69$, and $b_{\mathrm{LFRC}} = 400$. The Bode plot of the bandpass filter for the LFRC is shown in Fig. 7.

IV. ASPAC Algorithm and Modifications

The ASPAC algorithm is described in detail in [18,26]. In principle, the algorithm calculates a restricted control phase region in a stationary frame of reference, which is favorable for instability suppression, as shown in Fig. 8. First, the combustor instability pressure is sensed using a bandpass filter to isolate the instability frequency. The passband of the filter is based on some a priori knowledge of the approximate instability frequency, and its width covers the expected instability frequency drift within the operating range of an actual engine. The sensed pressure is phase shifted, with a phase that slides back and forth inside a restricted control region. This phase-shifted pressure is used to generate a command to the fuel valve which produces a fuel modulation opposing the instability pressure. The combustor pressure resulting from heat addition due to the fuel modulation, vectorially adds to the combustor pressure due to the instability to provide the overall dynamic combustor pressure. The dashed line region (so-called effective stability region) within the shaded area in Fig. 8 is the stable region in which the phase of the fuel modulation relative to the instability pressure is such that the power of the combustor pressure oscillations is reduced. The control vector slides back and forth within the effective control

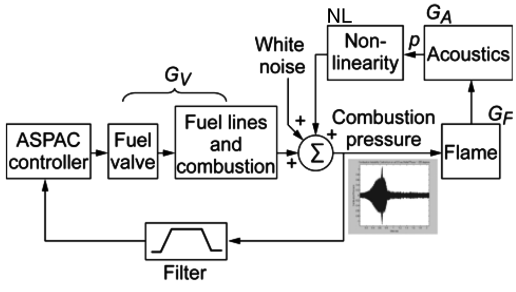

Fig. 5 Combustor instability control design block diagram.

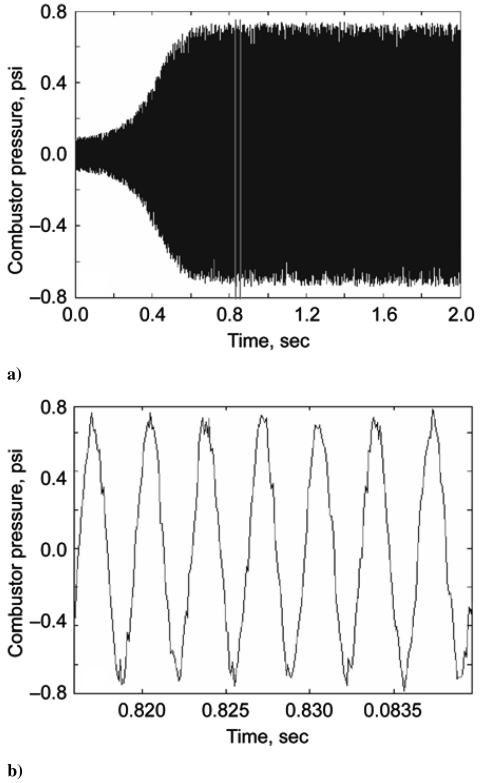

Fig. 6 Simulation of the self-excited combustion instability: a) self-excited instability time response, b) waveform of fully developed instability.

region: starting from one end of its boundary, marching to the other end, and then reversing direction.

One of the difficulties in this control problem is that the effective stability region continues to shrink as the instability is being suppressed and eventually disappears, rendering the system momentarily unstable. Normally, the stable region opens up again, control is restored, and the process repeats. Otherwise, a new control region is computed. Combustor noise plays a major role in this process in terms of how far the instability can be suppressed [2]. At higher suppression levels, the noise increasingly drives the process causing the instability phase to vary abruptly.

The pressure sensing and application of the control phase shift occurs at a rate of 10 KHz, which amounts to a phase resolution of approximately 18 deg for the HFRC instability. The controller calculates a new phase shift at a rate of 40 Hz. This slower control rate is due to the large dead time phase shift, which necessitates an

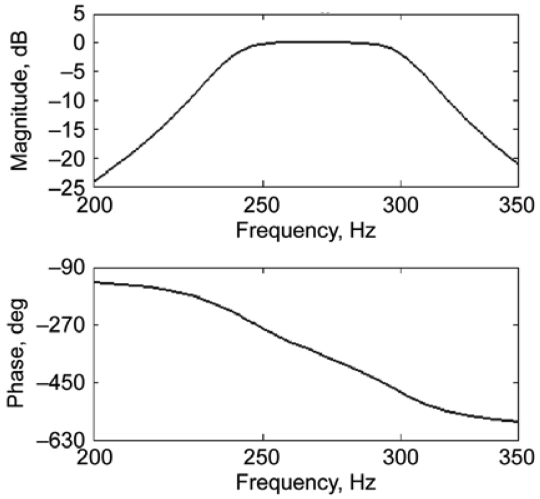

Fig. 7 Bode plot of bandpass filter for LFRC.

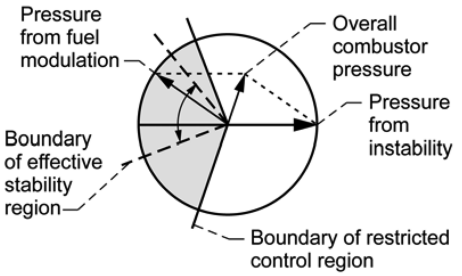

Fig. 8 ASPAC phasor diagram in a stationary frame of reference.

appropriately reduced controller bandwidth. Also, this controller optionally employs discontinuous exponential gain modulation control [18,26] (DEGMC). In this control mode, the gain is modulated on/off with an exponential decay to counteract the effective proportional gain variability produced by the large dead time phase delay of the plant. DEGMC was improvised for this particular application and is not a standardized control gain modulation technique. In addition, controller parameter adaptation [18,22] is employed to adapt some of the key parameters of the controller.

The control design was later modified to also include harmonic control [22]. The reason for this modification was evidence of coupling between the fundamental instability mode and its harmonics, identified by analyzing test results [2,18]. These types of coupling mechanisms, in the form of energy exchange between different frequency modes, have been reported in earlier works as well. Phillips [27], Kelly [28], and Zinn and Powell [29] provide mathematical treatments of the behavior. Harrje and Reardon [30], in a compilation of an extensive body of works with liquid propellant rocket combustion, also discuss nonlinear coupling behaviors.

Figures 9 and 10 show evidence of this coupling in the experimental combustor rig. The results in these two figures have been produced by certain manipulations of the test data described herein. Figure 9 shows the combustor rig pressure and the controlled fuel modulation command for the HFRC. Both signals are filtered to show only the instability and the respective control command. The fuel control command is shown opposing the instability, rather than the combustor pressure due to the fuel modulation, because the latter cannot be measured separately. However, this combustor pressure will be proportional to its control command displaced by a fixed phase. As a result, Fig. 9 was produced by sliding the time series of the control waveform relative to the overall combustor rig pressure, so that the phases of the two signals will be opposing at the regions where the instability pressure is decreasing (this much is known). This manipulation effectively changes the control signal to an approximation of its corresponding proportional combustor pressure. Even though the controlled signal phase starts opposing the combustion pressure soon after the pressure oscillations begin to grow again, the pressure oscillations continue to grow for a while, which persists beyond the time due to the large dead time delay of the plant. Additional analysis was done using experimental data obtained from the LFRC. Figure 10 shows the coherence of the instability harmonics using these data. One cannot compute the coherence of signals of different frequencies. Therefore, the original

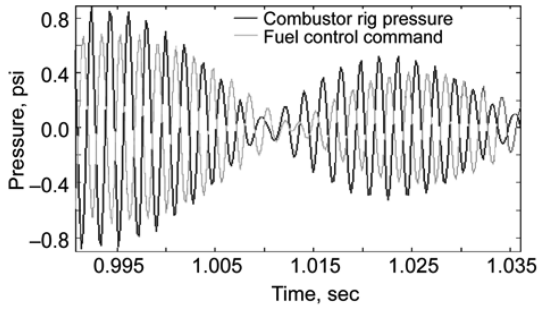

Fig. 9 Filtered combustor instability pressure versus filtered and phase-shifted fuel valve control command.

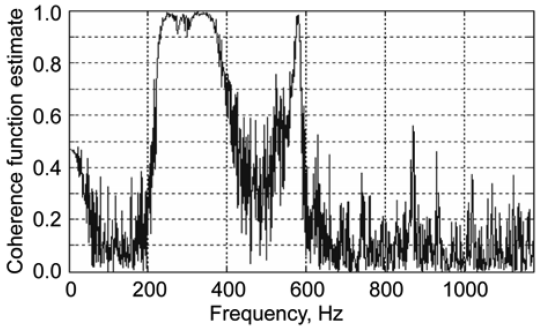

Fig. 10 Instability harmonics coherence plot.

combustor pressure signal was bandpass filtered to isolate the fundamental instability mode. Then, the original signal was also resampled to halve its frequency components. The resampled signal was again filtered to isolate the "fundamental mode" except, this time, the fundamental mode is actually the original second harmonic of the instability. Finally, the coherence of these two resulting signals was computed. This effectively gives the coherence between the fundamental and the second harmonic as seen in Fig. 10. As shown, the coherence between the second harmonic and fundamental (in the frequency band around 300 Hz) is high, around one, which suggests a coherent energy transfer between the fundamental and the harmonic. In Fig. 10, the coherences of some of the higher-order harmonics are shown as well because the bandpass filters do not completely get rid of the higher-order harmonics. The coherence suggested that additional suppression of the fundamental instability frequency may be possible by also simultaneously controlling the harmonics.

As a result of the previously discussed analysis, the controller structure was modified by adding a second harmonic control and third harmonic control to take advantage of the intraharmonic coupling effect. These modifications, which also include the parameter adaptation portion of the control algorithm, are shown in Fig. 11. The change with regard to harmonic control allows selecting the controller structure so as to focus on the fundamental and/or higher harmonics. The limitation of this control structure is the frequency which can be influenced by the fuel valve, that is, control can only be focused on the harmonic frequencies if the fuel valve has bandwidth/authority at those frequencies.

V. Controller Test Results

This section describes simulations and test results obtained using the ASPAC control methodology. Simulations were conducted initially to help develop the algorithm and to predict the controller behavior to the extent possible before the start of testing. Two separate tests were then conducted to validate the methodology. The first set of tests was carried out on the enginelike HFRC. The second test was performed on the LFRC.

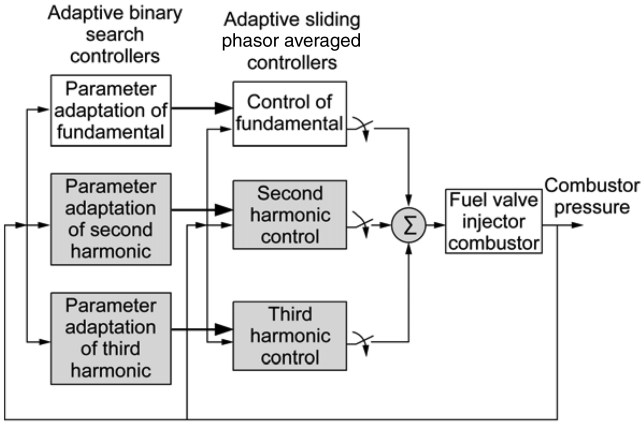

Fig. 11 ASPAC combustor instability control block diagram for harmonic control.

A. Simulations

Figure 12a shows the time response, and Fig. 12b shows the power spectral density of the combustor pressure with the combustor instability simulated using Eqs. (1–5). The instability is allowed to grow before control is applied at about 0.6 s. With no a priori knowledge of the phase required for suppression, the controller very briefly causes the instability to grow. The controller then quickly identifies the proper control phase to apply and suppresses the instability to reduce the instability pressure oscillations. Figure 12b shows the power spectral density when the controlled instability has been suppressed to about −50 dB (near the noise floor for this simulation), whereas the uncontrolled instability magnitude was about 0.6 psi or −4.4 dB. Brief control simulations were also conducted against a sectored 1-D physics-based model of the combustor process [31] to further validate the controls design.

B. HFRC Test Results

The objective of the HFRC control testing was to demonstrate control of combustor instability under conditions similar to those experienced in an actual aircraft gas-turbine engine (e.g., similar in terms of the operating conditions, instability frequency, and instability amplitude; see Fig. 2). As described earlier, the bandpass filter used in the simulation also simulates the large phase shift experienced in the combustor instability process. However, for rig testing, the filter design was changed to remove most of the phase shift shown in Fig. 7. Recall that the reasons for selecting the filter design for the simulation were to help isolate the instability frequency and also to simulate the process phase shift. As a result, a reduced phase-shift filter with a 450–700 Hz passband was selected for testing:

$$A = 1000\begin{bmatrix} -2.2627 & -1.6 & 3.51 & 0 \\ 1.6 & 0 & 0 & 3.51 \\ -3.51 & 0 & 0 & 0 \\ 0 & -3.51 & 0 & 0 \end{bmatrix}$$

$$B = [1600 \quad 0 \quad 0 \quad 0]^T; \qquad C = [0 \quad 1 \quad 0 \quad 0]$$

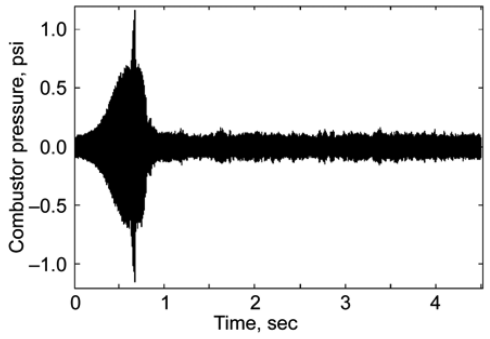

a)

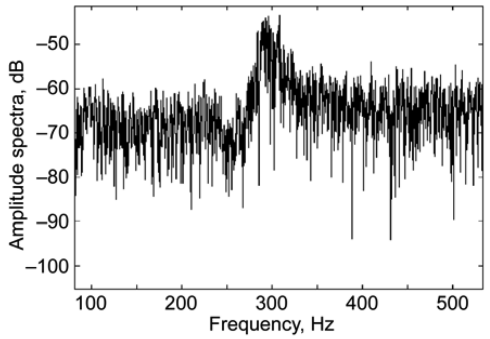

b)

Fig. 12 Simulation of combustor instability a) control response and b) power spectral density after instability suppression.

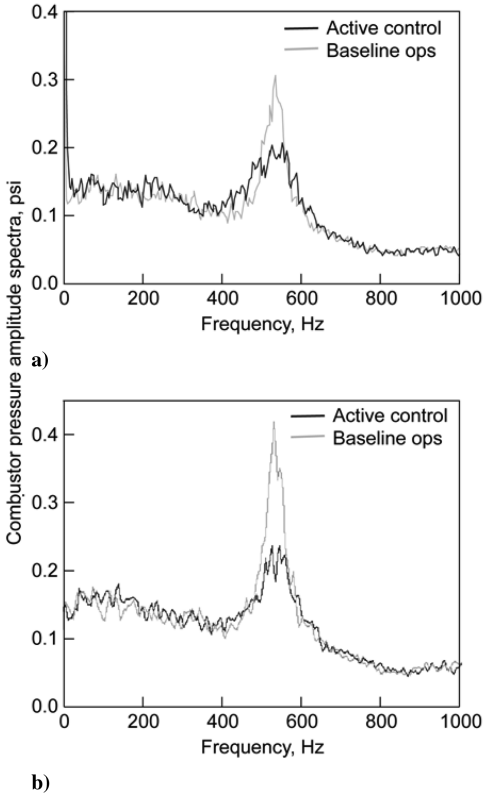

Fig. 13 Amplitude spectral density of uncontrolled versus controlled instability: a) earlier testing, b) later testing.

Through simulation and experimentation, it was found that best control results are achieved with a somewhat wide bandpass filter for both the HFRC and the LFRC (i.e., about 250 and 100 Hz passband, respectively).

Test results using the aforementioned control algorithm for the HFRC are shown in Fig. 13. Combustor pressure was sensed approximately 1-in. downstream from the fuel injector face using the previously described PCB dynamic pressure transducers. The fuel flow was modulated with the fuel valve. The control algorithm was implemented on a dSpace modular control system. The controller successfully suppressed the amplitude spectrum of the pressure oscillations at the instability frequency to near the noise floor. In terms of time domain reductions, the instability amplitude in the HFRC is small compared to the overall wideband noise (approximately one-seventh the noise amplitude) and no apparent reductions were visible in the time domain. As seen in the upper plot of Fig. 13, a lower-frequency coupling (∼5 Hz) existed in the combustor rig during initial testing. It was observed that occasional coupling between the combustor pressure and the facility open-loop fuel-feed

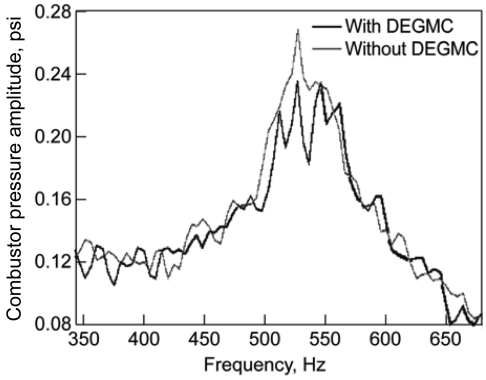

Fig. 14 Instability suppression with and without discontinuous exponential gain modulation control.

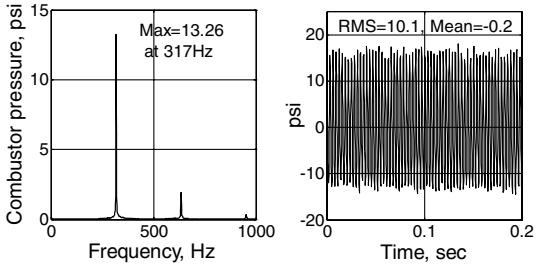

Fig. 15 Amplitude spectra and time domain of combustor pressure in the extended rig configuration (LFRC) with no active control applied.

pressure was causing the facility fuel pressure to oscillate at this low frequency. This was remedied for the second test through filtering and tuning of the mean fuel flow controller. The effect of using DEGMC, discussed in Sec. IV, was also investigated during these tests. Figure 14 shows test results with and without DEGMC. Some noticeable improvement (approximately 25% reduction) was observed by using the DEGMC portion of the algorithm. The results shown in Fig. 13b are with the DEGMC included in the controller.

C. Low Frequency Rig Configuration Test Results

The objective of the LFRC control testing was to demonstrate the control algorithm on a combustor rig with operating conditions similar to an actual aircraft gas-turbine engine, but with an instability which is more coherent (i.e., less damped) than that of the HFRC. This more closely approximates the instability coherence of the actual engine (see Figs. 2 and 3). Figure 15 shows the amplitude spectra of the combustor pressure (as shown earlier in Fig. 3), along with the time history of the instability pressure oscillations with no active control applied.

Initially, during testing with the LFRC, control was focused on just the fundamental frequency of the instability (∼315 Hz). Through this test, good control of approximately 90% suppression of the amplitude spectrum at the instability frequency was obtained, with a corresponding 35% reduction in time domain peak pressure oscillations, and a 70% reduction in rms pressure (see Fig. 16 compared with Fig. 15). In addition to the combustor instability pressure, Fig. 16 also shows the controller fuel valve command, in volts. As shown earlier, the fuel modulation command causes a modulation pressure in the combustor of approximately 1 psi/V up to about 350 Hz. For this test, approximately 20% fuel pressure modulation was required for instability suppression.

During the same test run, controller action was focused on the second harmonic. The purpose of this test was to see if the instability at the fundamental frequency responds to control of the second harmonic (as discussed earlier), to attempt additional instability suppression. It soon became apparent that the instability fundamental not only responded to the second harmonic control, but the suppression of the fundamental was more drastic than first expected.

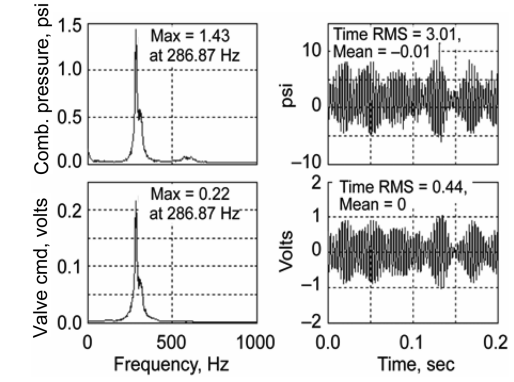

Fig. 16 Amplitude spectra and time domain of controlled instability pressure and control command with control focused on the fundamental instability frequency.

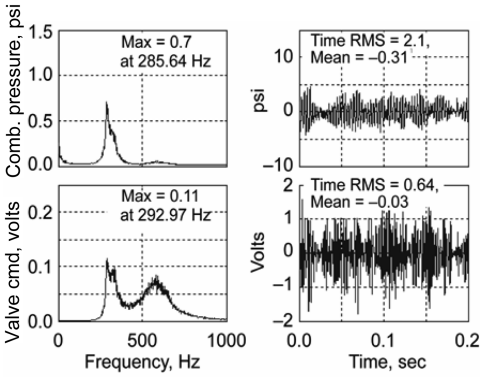

Fig. 17 Amplitude spectra and time domain of controlled instability pressure and control command with harmonic control applied: case 1.

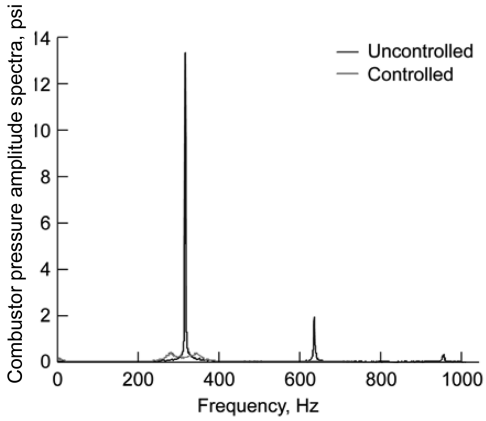

Fig. 19 Amplitude spectra of uncontrolled versus controlled instability pressure for the LFRC.

As shown in Fig. 17, the peak instability pressure amplitude is 0.7 psi. Comparing this result with the uncontrolled instability of Fig. 15 there is ∼95% suppression in amplitude at the instability frequency, a ∼75% reduction in time domain peak pressure oscillations, and an 80% reduction in rms pressure. The corresponding fuel valve command for this controlled combustor pressure is also shown in Fig. 17. From earlier frequency sweep testing, it had been observed that a 2 V peak-to-peak fuel valve excitation at 600 Hz was barely registering a noticeable pressure response (i.e., pressure above the noise floor). Therefore, the relatively little control authority at the second harmonic seems to be all that was needed to suppress the instability. The bandpass filter used to focus control effort on the second harmonic is wide enough to allow a small amount of effort at the fundamental. However, the higher-frequency control action is what seems to provide the improved results over the fundamental-only control.

The results from another control test, also focusing on the second harmonic, are shown in Fig. 18. For this test, parameter adaptations were enabled in the controller. These adaptations primarily included the controller gains and the parameters for the exponential gain modulation control. This result is even better in terms of the peak amplitude spectra than the result shown in Fig. 17 (0.39 versus 0.7 psi peak, 97 versus 95% amplitude suppression). In both tests, the second and higher harmonics of the instability have been almost completely eliminated. Some peak splitting is evident in this latter test. Depending on the particular controller design, evidence of peak splitting is more pronounced at increased levels of suppression, where combustor noise becomes more dominant and net random phase walks become more abrupt [2]. It is thought that this phenomenon could translate to frequency changes impacting energies at the instability side lobes. Comparisons of the uncontrolled (as in Fig. 15) versus the controlled instability for this last test (as in Fig. 18) are shown in Figs. 19 and 20.

Testing focusing on the third harmonic of the instability was also carried out during the course of this test run. However, based on this testing and from frequency sweep tests, very little fuel modulation authority of the fuel valve exists at the third harmonic of ∼945 Hz (no visible modulation authority is observable from frequency sweeps tests at these high frequencies). As a result, the third harmonic control testing was only able to reduce the instability by a few psi, down to about 8 psi peak pressure (results are not shown) at the instability frequency (as compared to >13 psi for the uncontrolled case).

The significance of second harmonic control is that better instability suppression seems to be achievable through this control, as the results presented here seem to support. The drawback is that harmonic control may require a higher fuel actuator bandwidth and possibly a penalty on the fuel actuator life due to higher cycling rates. Both problems could possibly be mitigated by the seemingly little actuator authority needed to suppress the instability by controlling the second harmonic, with correspondingly small magnitude dithering of the valve and small actuation rates. It could be possible that similar results may also be obtained by exercising subharmonic control or control at a significantly lower frequency than the instability. The next section will offer some discussions along these lines. Interaction with other instability modes (e.g., tangential modes) would be an interesting research subject as well, but was not investigated as part of this effort.

VI. Discussion of Results

Although the primary result of the effort reported in this paper is the successful suppression of combustion instability in an aircraft gas-turbine-engine-type combustor, a discussion of how this was accomplished (focusing control effort on the second harmonic) and why this was effective seems important as well. In this section, a possible explanation is offered for the mechanism that causes the phenomena of intraharmonic coupling in combustor instabilities. Also discussed is the possible role of impedances as a root cause of combustor instabilities. These discussions are based on the

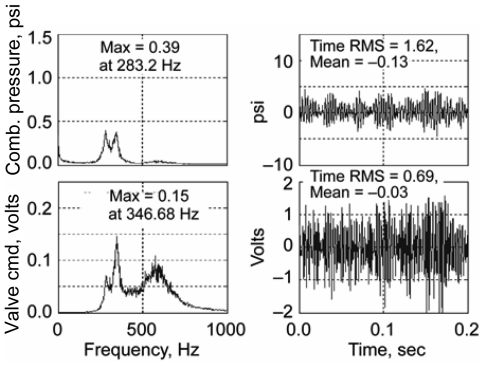

Fig. 18 Amplitude spectra and time domain of controlled instability pressure and control command with harmonic control applied: case 2.

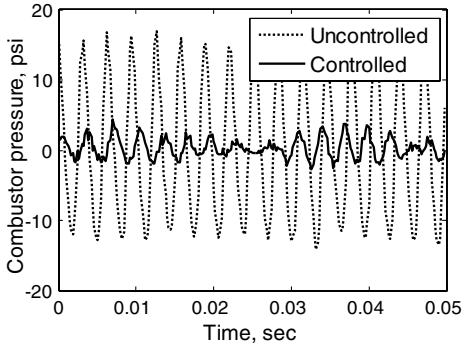

Fig. 20 Time domain of uncontrolled versus controlled instability for the LFRC. Controlled case is harmonic control, case 2.

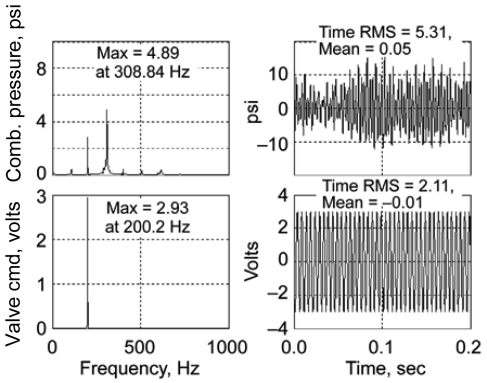

Fig. 21 Amplitude spectra and time history of combustor pressure after 10 min with 200 Hz fuel perturbation command applied.

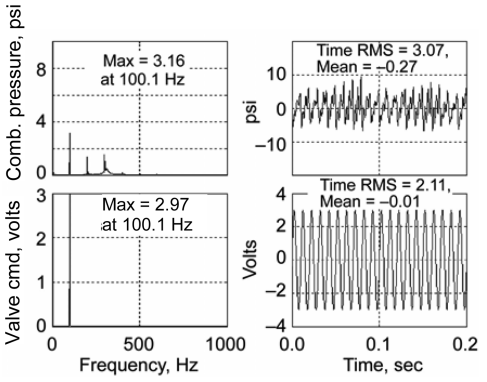

Fig. 23 Amplitude spectra and time history of combustor pressure with 100 Hz fuel perturbation command applied.

previously discussed instability control test results and also on other phenomena observed during testing.

In addition to closed-loop controls testing, additional test points were conducted where the combustor pressure was perturbed at various discrete frequencies and also where semicontinuous frequency sweeps were carried out. This was mainly done to characterize the fuel valve modulation authority. However, in the process of conducting these tests, some interesting phenomena were observed. Applying a discrete modulation of 2 or 3 V peak, at a lower frequency (in the range of 200 Hz), initially caused a barely visible response in the pressure amplitude spectra. But after about 10 min of fuel perturbation, this modulation would rapidly grow to greater than 2 psi in the combustor pressure (Fig. 21). This could be due to warming up of the fuel valve mechanism used to modulate the fuel or to some similar heating effect in the combustion process. Although not well understood, this increase in modulation capability was observed repeatedly, and so the discrete frequency excitation was included in the controller test procedure before turning the controller on. The growth of this discrete modulation also seemed to interact with the instability, reducing its peak somewhat. Further, discrete excitations at frequencies within a few hertz on either side of the instability frequency of approximately 315 Hz had an even more pronounced effect. Whereas the peak at the excitation frequency would grow significantly, the peak at the instability frequency would be reduced dramatically (Fig. 22). This latter effect can be explained by what can be called instability entrainment, whereby the system is susceptible to oscillations and will exhibit oscillatory behavior at frequencies near its resonance when excited at these frequencies, thereby increasing the system's energy at the driven frequency and at the same time reducing the energy at the resonant frequency.

Applying a discrete fuel modulation at frequencies below 200 Hz showed another interesting phenomenon. For a 100 Hz modulation frequency (but not at the 155 Hz half-frequency of the instability), a strong interference with the instability was observed (Fig. 23).

For all these open-loop modulation cases, it was observed that discrete frequency excitations seemed to create their own subharmonics, as well as harmonic frequencies. Overall, this combustor seemed to be very conducive to dynamic coupling between harmonics and also between discrete frequencies. As mentioned earlier, these types of dynamic couplings or nonlinearity effects have been described before in the areas of acoustics and liquid propellant rocket combustion [27–30]. One simple explanation for the couplings in gas-turbine engines between the fundamental instability and its harmonics (or other discrete frequencies) could be what is called wave asymmetry, observed in the discipline of oceanography [32]. For a combustor, the meaning of wave asymmetry here is that, when two or more pressure waves interfere, the interference is nonsymmetrical, causing a net suppression or amplification of the individual waves. This interference could, for example, be impacted by combustor noise (promoting amplification) and damping in the form of skin friction (promoting suppression). Eventually, a balance is reached where energy is exchanged, with one wave gaining and the other loosing some net energy. As described in [27], this energy transfer may be more efficient for certain wave number combinations.

Some of the unexplained experimental observations concerning the open- and closed-loop response to fuel modulation bring up the more fundamental topic of the root cause of combustor instabilities. The predominant explanation in the literature is that combustor instabilities are caused by thermoacoustic coupling, that is, coupling of the heat release with the acoustics of the combustor chamber. Based on this understanding, some experimenters have attempted to adjust the relative phase between the heat release and the acoustics by adjusting the fuel transport delay time to passively suppress the instability. This approach has had mixed results [33,34], which suggests that the relative phase is not the only mechanism responsible for the presence of an instability. In [2], it was discussed that, even though the thermoacoustics are responsible for providing the resonance that promotes pressure oscillations in the combustor chamber, the exact nature of the instability, like its magnitude and frequency, would seem to be the result of the fluidic impedances involved in this process (i.e., source/load-type impedance interactions). Impedances play a major role in the dynamic behavior of energy transfer systems, especially in systems that are not decoupled through choking of orifices. Therefore, a complete understanding or characterization of the instability behavior should not ignore the impedances involved in this process. This is becoming an area of investigation as reported in the literature, although mainly for premixed, gaseous-fueled gas turbines [35,36]. Gaining a more in-depth knowledge of the role that impedances play in this process, especially for liquid-fueled, aircraft gas-turbine-engine-type combustors, is of interest to the authors as a topic of future research, as it may allow for more effective control designs.

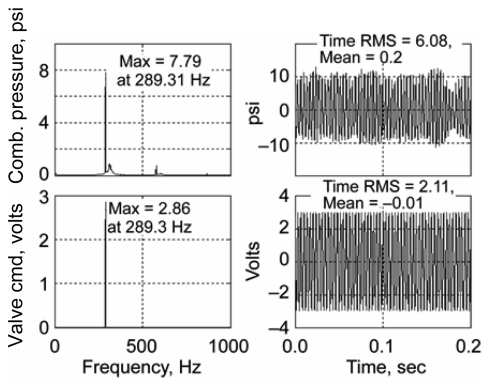

Fig. 22 Amplitude spectra and time history of combustor pressure with 289 Hz fuel perturbation command applied.

VII. Conclusions

This paper reports on test results of an adaptive control method for suppression of combustion instabilities. Results are presented from two different test runs. The first set of runs used a high-frequency

configuration of a combustor rig that emulates an aircraft gas-turbine engine combustor instability. The second set of test runs used a low-frequency configuration of the same rig. The test results validate the effectiveness of this adaptive control method in suppressing combustor instabilities in liquid-fueled gas turbines. Coupling between the fundamental mode of the instability and its harmonics was exploited to produce even higher suppression levels in the control of the instability. This was accomplished by focusing control at the second harmonic of the instability. A simple explanation has been offered for the mechanism involved in this coupling, which is attributed to wave asymmetry. Areas of interest for future research are to apply the demonstrated phase-shifting control method to advanced, low-emissions combustors; to develop actuation systems with more predictable dynamic response; and to develop a better understanding of the harmonic coupling effects and other instability mechanisms to support the development of even more effective control strategies (e.g., impedance-based control). Ultimately, the goal of these combustor instability control efforts is to enable NO_x emissions reductions through the application of advanced control approaches to ultralow-emissions, multipoint, lean, direct-injection combustors.

Acknowledgments

The authors gratefully acknowledge the technical contributions of Pratt and Whitney and United Technologies Research Center in providing the engine-traceable instability problem addressed in this paper, as well as critical modeling and testing support and technical consultation. The authors also acknowledge the contribution of the Georgia Institute of Technology in developing the high-frequency fuel modulation valve used for this effort. This work was supported by the NASA Smart Engine Components Program.

References

[1] Lefebvre, A. H., *Gas Turbine Combustion*, 2nd ed., Taylor and Francis, Philadelphia, 1999.

[2] Kopasakis, G., "Systems Characterization of Combustor Instabilities with Controls Design Emphasis," *AIAA 42nd Aerospace Sciences Meeting and Exhibit*, NASA TM 2004-212912, AIAA Paper 2004-0638, Jan. 2004.

[3] Lieuwen, C., and Zinn, B. T., "Investigation of Cycle-to-Cycle Variability in an Unstable Gas Turbine Combustor," American Society of Mechanical Engineers Paper 2000-GT-81, 2000.

[4] McManus, K. R., Poinsot, T., and Candel, S. M., "A Review of Active Control of Combustion Instabilities," *Progress in Energy and Combustion Science*, Vol. 19, No. 1, Feb. 1993, pp. 1–29. doi:10.1016/0360-1285(93)90020-F

[5] Dines, P. J., "Active Control of Flame Noise," Ph.D. Thesis, Cambridge Univ., Cambridge, England, U.K., 1984.

[6] Heckl, M. A., "Active Control of the Noise from a Rijke Tube," *Journal of Sound and Vibration*, Vol. 124, No. 1, July 1988, pp. 117–133.

[7] Sreenivasan, K. R., Raghu, S., and Chu, B. T., "The Control of Pressure Oscillations in Combustion and Fluid Dynamical Systems," AIAA Paper 1985-0540, 1985.

[8] Gleis, S., Vortmeyer, D., and Rau, W., "Experimental Investigation of the Transition from Stable to Unstable Combustion by Means of Active Instability Control," *Propulsion and Energetics Panel, 75th Symposium*, AGARD, Neuilly-sur-Seine, France, 1990, pp. 22:1–6.

[9] Dowling, A. P., Hooper, N., Langhorne, P. J., and Bloxsidge, G. J., "Active Control of Reheat Buzz," AIAA Paper 1987-433, 1987.

[10] Brouwer, J., Ault, B. A., Bobrow, J. E., and Sumuelsen, G. S., "Active Control for Gas Turbine Combustors," *23rd Symposium (International) on Combustion*, Combustion Inst., Pittsburgh, PA, 1990.

[11] Allgood, D., Campos-Delgado, D. U., Acharya, S., and Zhoo, K., "Acoustic Control of Thermoacoustic Instabilities Using Experimental Model-Based Controllers," American Society of Mechanical Engineers Paper GT2001-0518, 2001.

[12] Banaszuk, A., Ariyur, K. B., Krstic, M., and Jacobson, C. A., "An Adaptive Algorithm for Control of Combustion Instability," *Automatica*, Vol. 40, No. 11, pp. 1965–1972. doi:10.1016/j.automatica.2004.06.008, 2004.

[13] Cohen, J. M., Banaszuk, A., Hibshman, J. R., Anderson, T. J., and Alholm, H. A., "Active Control of Pressure Oscillations in a Liquid-Fueled Sector Combustor," *Journal of Engineering for Gas Turbines and Power*, Vol. 130, No. 5, 2008, pp. 2.1–2.8.

[14] Johnson, C. E., Neumeier, Y., Nuemaier, M., and Zinn, B. T., "Demonstration of Active Control of Combustion Instabilities on a Full-Scale Gas Turbine Combustor," American Society of Mechanical Engineers Paper GT2001-0519, 2001.

[15] Murugappan, S., Acharya, S., Park, S., Annaswamy, A. M., Ghoniem, A. F., Gutmark, E. J., and Allgood, D., "Optimal Control of Swirl-Stabilized Spray Combustion with System-Identification Approaches," *Combustion Science and Technology*, Vol. 175, No. 1, 2003, pp. 55–81. doi:10.1080/00102200302360

[16] Murugappan, S., Gutmark, E., Acharya, S., and Krstic, M., "Extremum-Seeking Adaptive Controller for Swirl-Stabilized Spray Combustion," *28th Symposium (Intl.) on Combustion*, Vol. 28, Combustion Inst., Pittsburgh, PA, July 2000, pp. 731–737.

[17] Barooah, P., Anderson, T. J., and Cohen, J. M., "Active Combustion Instability Control with Spinning Valve Actuator," *Journal of Engineering for Gas Turbines and Power*, Vol. 125, No. 4, 2003, pp. 925–932. doi:10.1115/1.1582495

[18] Kopasakis, G., "High Frequency Adaptive Instability Suppression Controls in a Liquid-Fueled Combustor," *AIAA 39th Joint Propulsion Conference and Exhibit*, NASA TM 2003-211805, AIAA Paper 2003-9581, 2003.

[19] Brouwer, J., Ault, B. A., Bobrow, J. E., and Sumuelsen, G. S., "Active Control for Gas Turbine Combustors," *Proceedings of the Combustion Institute*, Vol. 23, Combustion Inst., Pittsburgh, PA, 1991, pp. 1087–1092.

[20] Le, D. K., DeLaat, J. C., and Chang, C. T., "Control of Thermo-Acoustics Instabilities: The Multi-Scale Extended Kalman Approach," AIAA Paper 2003-4934, NASA TM 2003-212536.

[21] Cohen, J., Proscia, W., and DeLaat, J., "Characterization and Control of Aeroengine Combustion Instability: Pratt & Whitney and NASA Experience," *Combustion Instabilities in Gas Turbine Engines: Operational Experience, Fundamental Mechanisms, and Modeling*, edited by T. Lieuwen, and V. Yang, AIAA, Reston, VA, 2005, pp. 113–145.

[22] Kopasakis, G., DeLaat, J. C., and Chang, C. T., "Validation of an Adaptive Combustion Instability Control Method for Gas-Turbine Engines," *AIAA 40th Joint Propulsion Conference and Exhibit*, NASA TM 2004-213198, AIAA Paper 2004-4028, 2004.

[23] Cohen, J. M., Hibshman, J. R., Proscia, W., Rosfjord, T. J., Wake, B. E., McVey, J. B., Lovett, J., Ondas, M., DeLaat, J., and Breisacher, K., "Experimental Replication of an Aeroengine Combustion Instability," NASA TM 2000-210250, 2000.

[24] DeLaat, J. C., Breisacher, K. J., Saus, J. R., and Paxson, D. E., "Active Combustion Control for Aircraft Gas Turbine Engines," NASA TM 2000-210346, AIAA Paper 2000-3500, 2000.

[25] Vaudrey, M. A., Baumann, W. T., and Saunders, W. R., "Time-Averaged Gradient Control of Thermoacoustic Instabilities," *Journal of Propulsion and Power*, Vol. 19, No. 5, Sept.–Oct. 2003, pp. 830–836. doi:10.2514/2.6172

[26] Kopasakis, G., and DeLaat, J. C., "Adaptive Instability Suppression Controls in a Liquid-Fueled Combustor," *AIAA 38th Joint Propulsion Conference and Exhibit*, NASA TM 2002-211805, AIAA Paper 2002-4075, 2002.

[27] Phillips, O. M., "On the Dynamics of Unsteady Gravity Waves of Finite Amplitude," *Journal of Fluid Mechanics*, Vol. 9, No. 2, 1960, pp. 193–217. doi:10.1017/S0022112060001043

[28] Kelly, R. E., "On the Resonant Interaction of Neutral Disturbances in Two Inviscid Shear Flows," *Journal of Fluid Mechanics*, Vol. 31, Pt. 4, 1968, pp. 789–799. doi:10.1017/S0022112068000479

[29] Zinn, B. T., and Powell, E. A., "Nonlinear Combustion Instability in Liquid-Propellant Rocket Engines," *Thirteenth Symposium (International) on Combustion*, Combustion Inst., Pittsburgh, PA, 1970, pp. 491–504.

[30] Harrje, D. T., and Reardon, F. H., "Liquid Propellant Rocket Combustion Instability," NASA SP-194, 1972.

[31] Paxson, D. E., "A Sectored One-Dimensional Model For Simulating Combustion Instabilities in Premix Combustors," *AIAA 38th Aerospace Sciences Meeting and Exhibition*, NASA TM 1999-209771, AIAA Paper 2000-0313, 2000.

[32] Shuvalov, V. V., "Mechanisms of Tsunami Generation by Impacts," Inst. for Dynamics of Geospheres, Russian Academy of Science, Moscow, p. 119334

[33] Straub, D. L., and Richards, G. A., "Effect of Fuel Nozzle Configuration on Premix Combustion Dynamics," *International Gas Turbine & Aeroengine Congress & Exhibition*, American Society of Mechanical

Engineers Paper 98-GT-492, 1996.
[34] Lee, J. L., Kim, K., and Santavicca, D. A., "A Study of the Role of Equivalence Ratio Fluctuations During Unstable Combustion in a Lean Premixed Combustor," *AIAA 39th Joint Propulsion Conference and Exhibit*, AIAA Paper 2003-4015, July 2002.
[35] Richards, G., and Straub, D., "Control of Combustion Dynamics Using Fuel System Impedance," *ASME Turbo Expo 2003*, American Society of Mechanical Engineers Paper GT2003-38521, June 2003.
[36] Richards, G. A., and Robey, E. H., "Effect of Fuel System Impedance Mismatch on Combustion Dynamics," *Journal of Engineering for Gas Turbines and Power*, Vol. 130, No. 1, 2008, pp. 011510.1–011510.7. doi:10.1115/1.2771249

D. Talley
Associate Editor